An efficient steady-state thermal model for predicting the lack-of-fusion porosity during laser powder bed fusion process

JIA Yabo[1,2,a] *, SAADLAOUI Yassine[3,b], and BERGHEAU Jean-Michel[3,c]

[1]Univ. Polytechnique Hauts-de-France, CNRS, UMR 8201 - LAMIH - Laboratoire d'Automatique de Mécanique et d'Informatique industrielles et Humaines, F-59313, Valenciennes, France

[2]INSA Hauts-de-France, F-59313, Valenciennes, France

[3]Univ. Lyon, ECL-ENISE, CNRS, UMR 5513 – LTDS, F-42023 Saint-Etienne, France

[a]yabo.jia@uphf.fr, [b]yassine.saadlaoui@enise.fr,[c]jean-michel.bergheau@enise.fr

Keywords: Steady-State Model, Lack-Of-Fusion, Laser Powder Bed Fusion

Abstract. The lack-of-fusion porosity due to the incomplete melting of the powder should be avoided during laser powder bed fusion (LPBF) process. The porosity will reduce the performance of mechanical properties. In certain manufacturing processes, the thermal and metallurgical quasi-steady-state can be reached quickly. In this article, a steady-state model, incorporating new dedicated boundary conditions, is proposed and applied in the multi-track simulation of LPBF to control porosity. Various processing parameters, such as hatching space and cooling time inter-pass can be investigated. The transient step-by-step simulation is also employed as the numerical reference. Numerical comparisons demonstrate that the proposed steady-state model achieves a relative good agreement with the numerical reference while significantly reducing computing time (2-3 minutes).

Introduction

The lack-of-fusion porosity due to the incomplete melting of the powder should be avoided during laser powder bed fusion (LPBF) process. The part porosity will reduce the performance of mechanical properties. Traditionally, controlling the presence of such defects involves experimental trial-and-error tests to optimize fabrication parameters. However, conducting experimental studies for testing a large number of parameters can be extremely costly.

To mitigate the presence of such defects, various numerical models have been employed to simulate Laser Powder Bed Fusion (LPBF), including geometrical models [1] and analytical models [2]. However, these models lack predictability due to the absence of certain physical properties. In contrast, some multiphysics models [4] exhibit predictability, but their computational cost is prohibitive for multi-track simulations. A transient step-by-step heat-transfer simulation offers a good compromise. Nevertheless, its computational cost remains too high for multi-track and multi-layer simulations. Recently, JIA et al. [5] provides a comprehensive review of different modeling strategies of multiphysics and multi-scales applied in powder-based metallic additive manufacturing processes.

In certain manufacturing conditions (constant scanning speed, constant energy input, etc.), the thermal quasi-steady-state can be reached very quickly. Therefore, a steady-state thermal model based on new dedicated boundary conditions has been proposed and applied in the simulation of LPBF [3], which is much more computational efficient than transient step-by-step simulation. Meanwhile, this proposed steady-state model possibly considers temperature-dependent material properties, Gaussian distribution of heat source, convective and radiative heat losses, powder-compact transition, enthalpy due to solid-liquid transition, and effect of heat convection in the melt pool, while allowing fast and accurate predictions of the melt pool size and steady-state temperature distribution. Single-track LPBF simulations were conducted for two widely used

materials, namely AlSi10Mg and Inconel 718. The melt pool sizes simulated by the proposed model were compared with those obtained from a transient model as well as experimental results, specifically the melt pool morphology. The relative error observed for all the numerical and experimental validation tests was less than 5%.

In the current contribution, the single-track steady-state thermal model is extended to multi-tracks simulation. The proposed multi-track steady-state thermal model will be used to investigate the presence of lack-of-fusion with different scanning speed, powder layer thickness and hatch spacing, which allows reduce the number of expensive trial and error experimental tests.

Numerical models

The proposed multi-tracks model is based on single-track steady-state model presented in [4], which has been successfully applied to LPBF simulations with two most used materials (AlSi10Mg and Inconel 718). A perfect correlation has been observed compared with the experimental results. Below is a concise introduction to the single-track steady-state model based on new dedicated boundary conditions.

The steady-state heat transfer problem is governed by a convection-diffusion equation (refer with: Eq. 1), with the underlying assumption of infinite length in the direction of the moving heat source.

$$\rho C \mathbf{W} \cdot \mathbf{grad}T = \mathbf{div}(\lambda \, \mathbf{grad}T) + q \tag{1}$$

where $\lambda = \sum_{state} p_i \lambda_i$ with p_i, λ_i corresponding to the proportion and thermal conductivity of each state i (powder or compact). The state transformation (powder to bulk) is controlled by the temperature, and this transformation is invertible once the temperature exceeds the melting temperature. C represents the heat capacity and q is heat source term used to describe the interaction between powder bed and laser beam. A constant density value at room temperature is employed in the current study since no mass conservation equation is solved. The latent heat effect related to solid-liquid transformation can be modeled by apparent heat capacity method [6].

The powder bed is modeled as a continuum medium with thermal properties differing from the compact state ($\lambda_c(T)$) [8]. The thermal conductivity of powder bed ($\lambda_p(T)$) is defined as follows:

$$\lambda_p(T) = \begin{cases} \lambda_c(T)(1-\varphi)^n & for \ T = 293K \\ \dfrac{\lambda_c(T_m - \lambda_p(293K))}{T_m - 293K}(T - 293K) + \lambda_p(293K) & for \ 293K < T < T_m \\ \lambda_c(T) & for \ T > T_m \end{cases}$$

here, φ represents the porosity of the powder bed, and n is an empirical parameter. T (in Kelvin) corresponds to the temperature of the powder, with T_m being the melting temperature.

To conduct a steady-state heat transfer simulation with a short geometry, novel dedicated boundary conditions are introduced for the steady-state model [4]. These conditions are derived from an analytically inspired solution of the 1D heat transfer equation outside the mesh. A Fourier-type condition is imposed on the downstream and upstream surfaces (2D element) to emulate the heat exchange between the considered geometry and the volume beyond it. These new boundary conditions are presented as follows:

- Upstream surface: $\lambda \dfrac{dT}{dn} = \lambda(\beta - \alpha)(T_0 - T(up))$

- Downstream surface: $\lambda \dfrac{dT}{dn} = \lambda(\alpha + \beta)(T_0 - T(down))$

where $\alpha = -\frac{\rho CW}{2\lambda}$ and $\beta = \frac{\sqrt{4K\lambda + (\rho CW)^2}}{2\lambda} = \sqrt{\alpha^2 + \frac{K}{\lambda}}$ with $K = H\frac{P}{S}$. H is the heat exchange coefficient (simply equal to h_c). P is the perimeter, and S is the surface of upstream surface. T_0 is the temperature ambient, and $T(up)/T(down)$ is the temperature at upstream/downstream surface. More information can be found in [4].

The convective (Q_c) and radiative (Q_r) losses at free surface are modeled by Newton's law:

$$Q_c = h_c(T - T_0)$$

$$Q_r = \sigma\varepsilon(T^4 - T_0^4)$$

where h_c, σ and ε are the coefficient exchange with air, Stefan-Boltzmann constant, and surface emissivity, respectively. T and T_0 are in Kelvin.

All the development and simulations are performed in $SYSWELD^{TM}$ [7].

Numerical example

In this section, a numerical example is prepared to highlight the computational efficiency of proposed multi-track steady-state model. In the multi-track simulations, both transient step-by-step and proposed steady-state models are employed, and the transient step-by-step simulation is considered as the numerical reference. Since the quality of numerical results predicted by $SYSWELD^{TM}$ have been verified and confirmed by lots of researchers, no further validations tests will be conducted in the current studies.

In the current study, the material properties of 316L are utilized, and the properties in both powder and bulk states are presented in Table 1. The material properties of the bulk state are sourced from the SYSWELD database [7]. It's important to note that the density of the powder state is considered equal to that of the bulk state, as the volume shrinkage due to the transformation from powder state to bulk state is not taken into account. The thermal conductivity of powder bed is calculated from aforementioned equation with φ=0.7 and n=4. Numerical experience indicates that the thermal conductivity difference between the two states should not be excessively large. Otherwise, convergence issues may arise, or an extremely small time step might be required. The specific values of powder bed are the same as the bulk state.

Table 1. material properties of 316L

State	Properties	20°C	400°C	900°C	1400°C	1800°C
powder	Density (kg/mm^3)			$7.72 * 10^{-6}$		
	Thermal conductivity (W/mm.K)	0.00357	0.0104	0.01941	0.02842	0.02842
	Specific heat (J/kg.K)	494.1	578.0	635.5	799.8	799.8
bulk	Density (kg/mm^3)			$7.72 * 10^{-6}$		
	Thermal conductivity (W/mm.K)	0.01488	0.02056	0.02769	0.02842	0.02842
	Specific heat (J/kg.K)	494.1	578.0	635.5	799.8	799.8

Figure 1 presents the geometry, mesh and process information, and the powder bed is of 40 μm. The model width (W), depth (D), length (L) are 2mm, 1mm, 1.5mm respectively. The simulation consists of 7 tracks with hatch spacing of 200 μm, and scanning speed is set of 100 mm/s. The cooling time between two successive track is of 0.005s. The 3D mesh is generated by translation of 2D mesh (Figure 1-(C)), and all the layers in scanning direction are equal to 10 μm. This model contains about 433k nodes and 462k 3d elements.
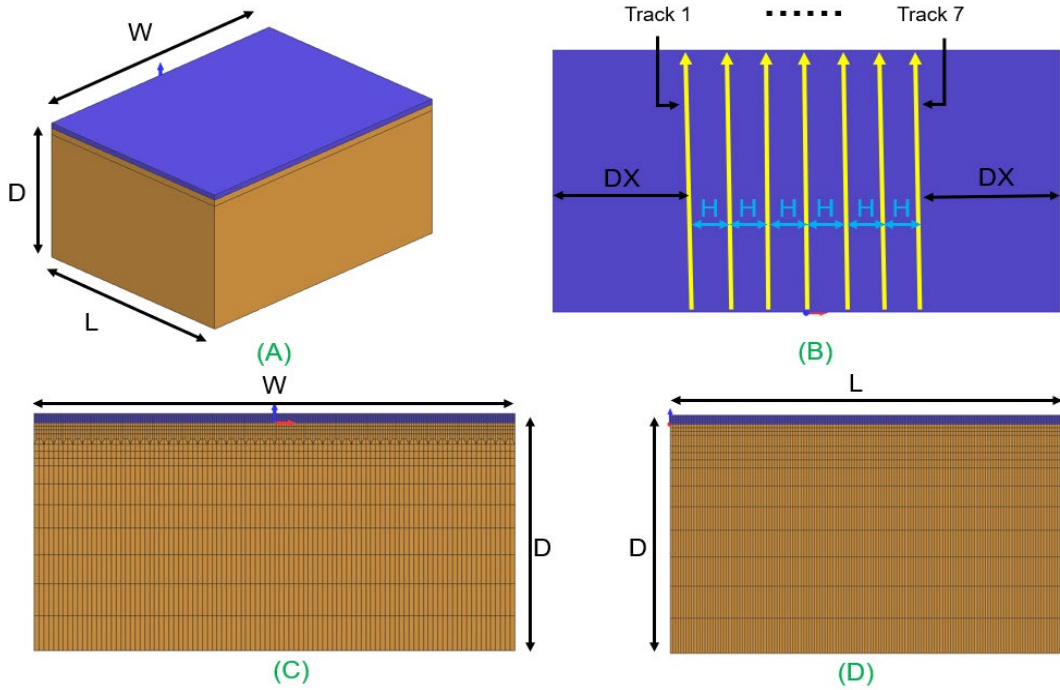

Fig.1, the geometry and mesh information for transient simulation

The geometry of steady state model is shown in figure 2, and the 3D mesh topology is created with same as manner as the transient model. Compared to transient model, the steady-state model has the same width and depth, while the length is only of 0.6mm. Solving steady-state problem with convection-diffusion equation and a short geometry can greatly reduce the CPU time. The position of heat source is at center of its trajectory.
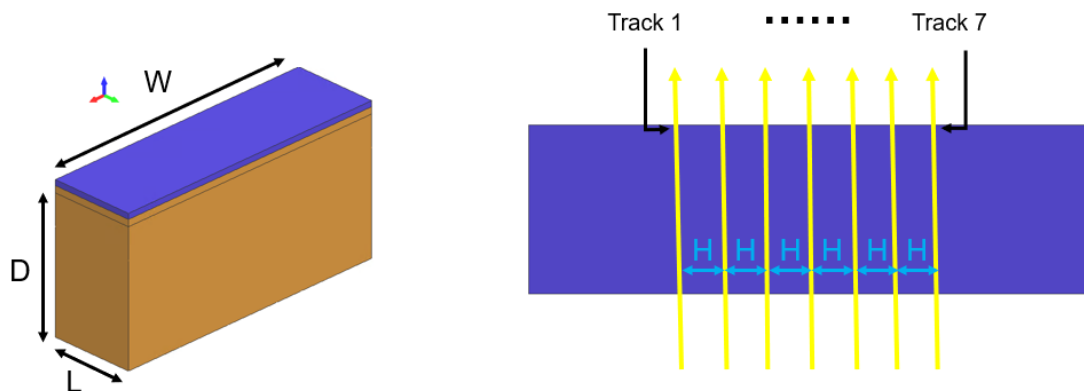

Fig.2, the geometry for steady-state simulation

A 2D heat source is applied to simulate interaction between laser and powder bed (see reference [3]). The heat source is described by the following equation:

$$Q = \frac{P}{\pi R_0^2} \exp\left(\frac{-R^2}{R_0^2}\right)$$

where R represent the relative position between the gauss point and center of heat source. R_0 is the radius of laser beam. P is effective energy absorbed by powder bed. In the current study, R_0 is 50 μm, and P is 40 W.

Table 2 presents a comparison of simulated melt pool size. The melt pool size stabilizes rapidly after track 1 for the steady-state simulation, which means that only the precedent deposited track will affect the prediction of actual track. However, the melt pool size given by transient model increase, which can be explain by the fact of heat cumulation. In comparison, the steady-state model provides a good correlation for the first track, but discrepancies become more significant with subsequent depositions. This growing difference is attributed to the omission of heat cumulation effects in the steady-state model. The steady-state model is about 150 time more efficient than transient model in terms of CPU time, which requires only 2 minutes in place of 5 hours.

Table 2. comparison of simulated melt poo size

Dimension	Type of simulation	Track 1	Track 2	Track 3	Track 4	Track 5	Track 6	Track 7
Width (μm)	Steady-state	217	204	204	204	204	204	204
	Transient	210	213	218	221	222	223	224
Depth (μm)	Steady-state	84	82	82	82	82	82	82
	Transient	81	86	88	92	93	96	99
Length (μm)	Steady-state	268	266	266	266	266	266	266
	Transient	270	282	286	294	310	310	310

Figure 3 provide the comparison of temperature distribution given by transient and steady-state model. The steady-state model cannot consider the effect of heat accumulation in the multi-track simulations, which lead to under-estimation of melt pool size. The figure 3 confirms again this conclusion.
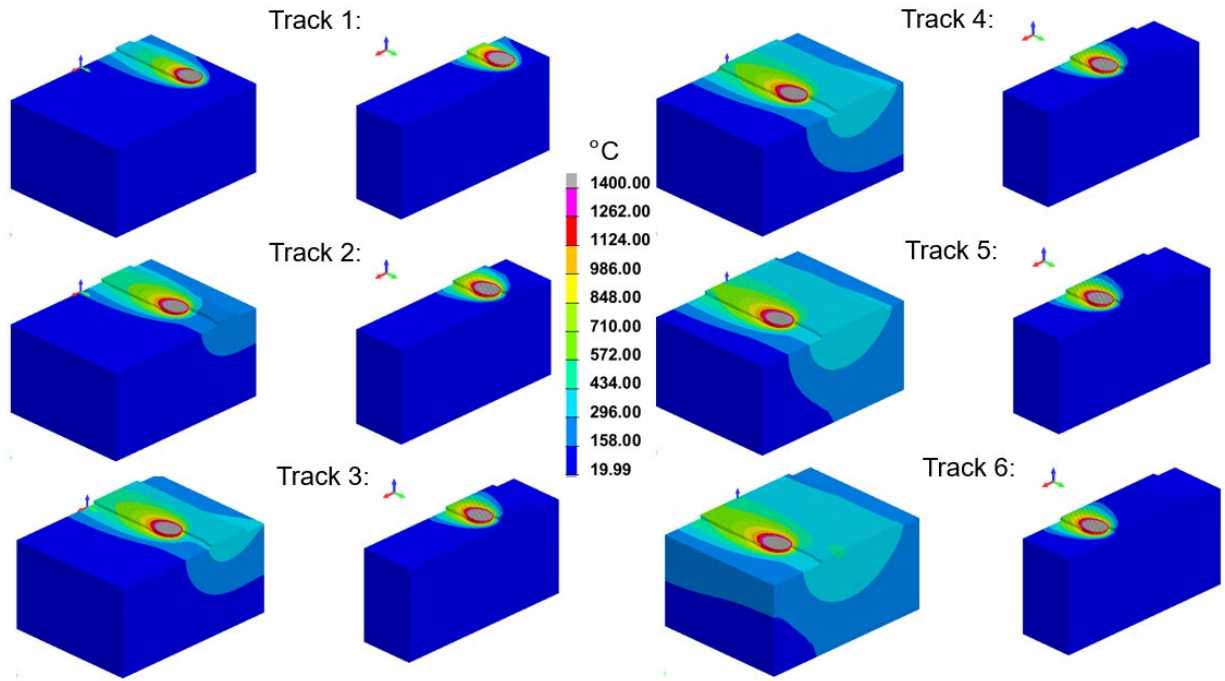
Fig.3, temperature distribution given by transient and steady-state model

Figure 4 shows the comparison of melting profiles given by these two models, and the temperature presented here is the maximal temperature at each node during the process. We can remark that the melt pool enlarges progressively in the transient model because of heat cumulation. However, the melt pool of each track predicted by steady-state model is almost the same. The lack of fusion can be observed in both cases. Furthermore, since the steady-state model tends to slightly underestimate the melt pool size, the parameters suggested by the steady-state model provide more reliability.
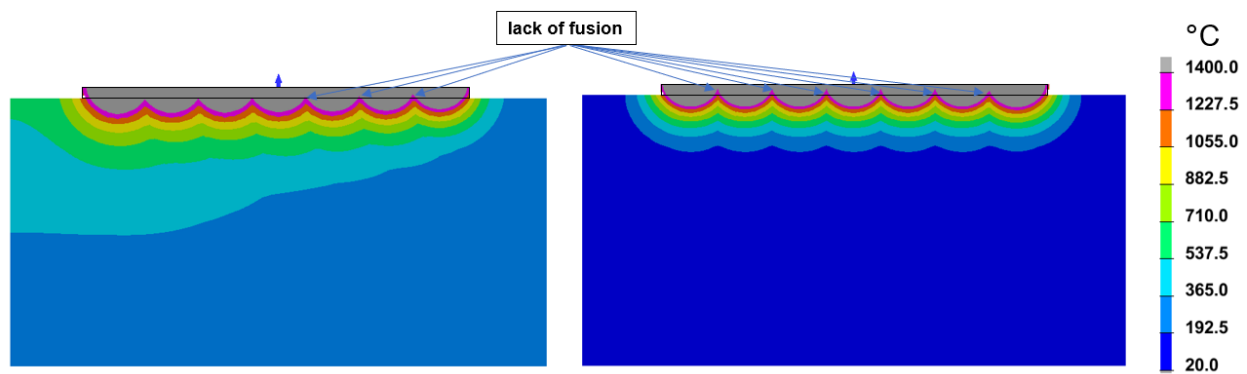

Fig.4, comparison of melting profile given by transient model (left) and steady-state model (right)

To avoid the presence of porosity, the steady-state model is employed to optimize different hatch spacing. Therefore, the hatch spacing of 200 μm, 190 μm, 180 μm, 170 μm are tested, and figure 5 shows the simulated fusion profiles. The comparisons shows that a hatch spacing of 170 μm should be adopted.
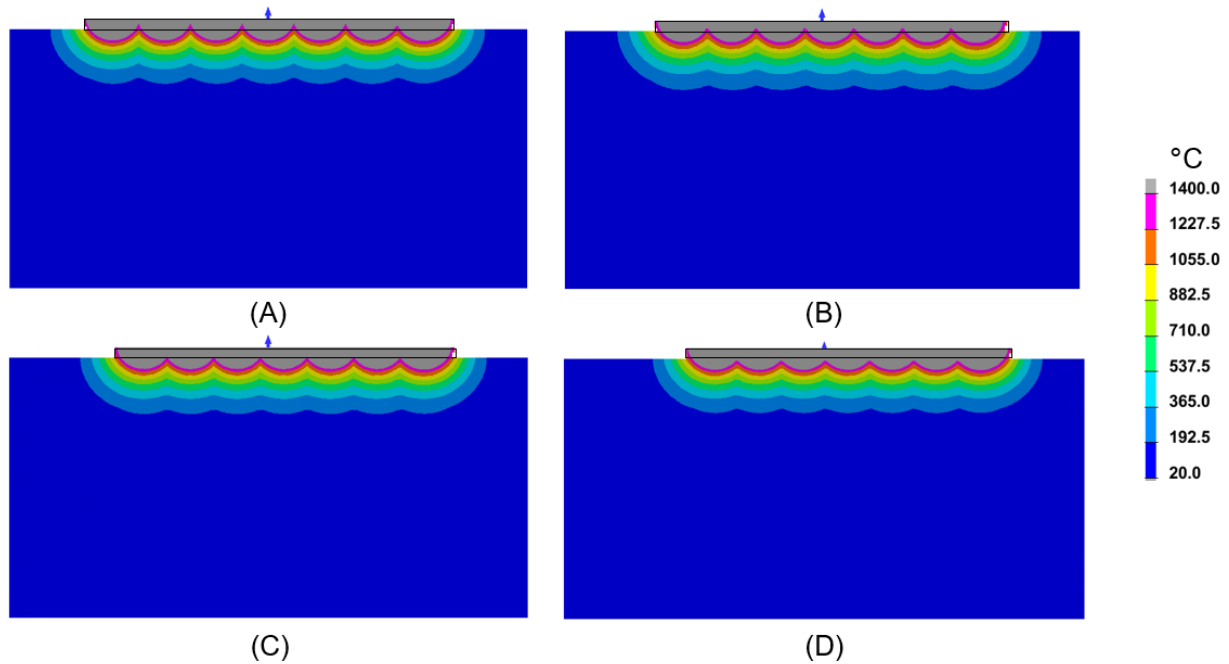
Fig.5, fusion profile with different hatch spacings: (A) 200 μm, (B) 190 μm, (C) 180 μm, (D)170 μm

Conclusion

This article presents the first tentative of applying steady-state model to multi-track simulation. The numerical results are compared against the transient model, and a relative error less than 18% has been observed in the comparison of simulated melting pool size. Moreover, the steady-state model highlights its extremely high computational efficiency, which can be beneficial for optimizing the fabrication parameters to avoid the presence of porosity. To improve the prediction of steady-state model, the next step is to incorporate the heat cumulation effect. Moreover, it would be also interesting to consider the phase transformation (perlite, austinite, etc.) for the multi-track simulations.

References

[1] TANG, Ming, PISTORIUS, P. Chris, et BEUTH, Jack L. Prediction of lack-of-fusion porosity for powder bed fusion. Additive Manufacturing, 2017, vol. 14, p. 39-48. http://dx.doi.org/10.1016/j.addma.2016.12.001

[2] NING, Jinqiang, WANG, Wenjia, ZAMORANO, Bruno, et al. Analytical modeling of lack-of-fusion porosity in metal additive manufacturing. Applied Physics A, 2019, vol. 125, p. 1-11.

[3] JIA, Yabo, SAADLAOUI, Yassine, ROUX, Jean-Christophe, et al. Steady-state thermal model based on new dedicated boundary conditions–application in the simulation of laser powder bed fusion process. Applied Mathematical Modelling, 2022, vol. 112, p. 749-766. https://doi.org/10.1016/j.apm.2022.08.013

[4] JIA, Yabo, SAADLAOUI, Yassine, FEULVARCH, Eric, BERGHEAU, Jean-Michel. An efficient local moving thermal-fluid framework for accelerating heat and mass transfer simulation during welding and additive manufacturing processes. Computer Methods in Applied Mechanics and Engineering, 2023, vol. 419, p. 116673. https://doi.org/10.1016/j.cma.2023.116673

[5] JIA, Yabo, NACEUR, Hakim, SAADLAOUI, Yassine, DUBAR, Laurent, BERGHEAU, Jean-Michel. A comprehensive comparison of modeling strategies and simulation techniques applied in

powder-based metallic additive manufacturing processes. Journal of Manufacturing Processes, 2024, vol 110, p. 1-29. https://doi.org/10.1016/j.jmapro.2023.12.048

[6] BONACINA, Comini, COMINI, G., FASANO, A., et al. Numerical solution of phase-change problems. International Journal of Heat and Mass Transfer, 1973, vol. 16, no 10, p. 1825-1832.

[7] Software SYSWELD version 2023, ESI-Group, Lyon, France, 2023.

[8] Loong-Ee Loh, Chee-Kai Chua, Wai-Yee Yeong, Jie Song, Mahta Mapar, Swee-Leong Sing, Zhong-Hong Liu, Dan-Qing Zhang. Numerical investigation and an effective modelling on the Selective Laser Melting (SLM) process with aluminium alloy 6061. International Journal of Heat and Mass Transfer, 2015, vol 80, p.288-300, https://doi.org/10.1016/j.ijheatmasstransfer.2014.09.014